

Efficient Visible Quasi-2D Perovskite Light-Emitting Diodes

Jinwoo Byun, Himchan Cho, Christoph Wolf, Mi Jang, Aditya Sadhanala, Richard H. Friend, Hoichang Yang, and Tae-Woo Lee*

Organic/inorganic hybrid perovskites (hereafter, denoted as perovskites) are light-emitting materials that have many advantages as components of light-emitting diodes (LEDs).^[1,2] Organic/inorganic hybrid perovskite LEDs (PeLEDs) can provide wide color range due to their narrow spectral width (full width at half maximum (FWHM) \approx 20 nm).^[2] Perovskites are solution-processable with low-cost materials,^[3] and their color of the emitting light can be easily tuned by changing the halide component.^[2]

However, the efficiency of PeLEDs is intrinsically limited by facile dissociation of excitons in perovskites due to their long exciton diffusion length^[4] and small exciton binding energy.^[5] Therefore, to increase the efficiency of PeLEDs, a larger exciton binding energy and a shorter exciton diffusion length are needed. Recently, we reported that efficiency of PeLEDs can be highly enhanced by reducing grain size and thus achieving small exciton diffusion length.^[6]

Substituting cations in perovskites is a promising way to reduce exciton diffusion length and increase exciton binding energy. By substituting the methyl ammonium (MA) cations with larger organic ammonium (OA) cations, the crystal structures of perovskites change to 2D layered structures,^[7] where excitons are more strongly confined to inorganic layers, increasing exciton binding energy more than 200 meV.^[8] However, achieving high-efficiency PeLEDs using 2D perovskites is difficult because charge transport is inhibited at low voltages by enlarged insulating OA groups. To retain decent charge transport property without losing exciton confinement effect, quasi-2D perovskites can be formed by mixing 3D (based on MA cations) and 2D (based on larger OA cations) structure perovskites.^[9] However, visible PeLEDs based on quasi-2D perovskites have not been reported. Furthermore, an in-depth study of electronic and optical properties of quasi-2D perovskites is imperative.

In this work, we have studied how to enhance the luminescent properties of perovskite films and the efficiency of PeLEDs by using quasi-2D structure. Quasi-2D perovskites have both 3D and 2D perovskite crystal structure (Figure 1). By mixing phenylethyl ammonium (PEA) lead bromide ((C₆H₅C₂H₄NH₃)₂PbBr₄, (PEA)₂PbBr₄) with MAPbBr₃, we achieved a uniform perovskite film morphology with a reduced particle size (Figure S1, Supporting Information). We found that PEA₂MA_{m-1}Pb_mBr_{3m+1} ($m = 1-4$, integer) films consist of several different quasi-2D structures, and the energy transfer occurs from the crystals with larger bandgap to those with smaller bandgap, making recombination occurs only in the crystals with the smallest bandgap. Efficient quasi-2D PeLEDs (current efficiency = 4.90 cd A⁻¹) were realized and the origins of the efficiency enhancement were analyzed using film morphology, trap density of states (tDOSs), photoluminescence (PL) quantum efficiency (PLQE) and PL lifetime. To the best of our knowledge, these are the first visible PeLEDs based on quasi-2D perovskites.

Quasi-2D perovskite structure (OA)₂(MA)_{m-1}Pb_mBr_{3m+1} ($m = 1-4$, integer) can be classified according to the number of PbI₆ layers sandwiched between two OA layers.^[10] We prepared quasi-2D perovskite films and determined the dimension of the films by conducting UV-vis absorption spectroscopy. We used two different precursor solutions: 40 wt% MAPbBr₃ solution and 10 wt% (PEA)₂PbBr₄, which are dissolved in dimethylformamide (DMF) and mixed in various MAPbBr₃:(PEA)₂PbBr₄ volume ratios (1:0 [MAPbBr₃], 1:2–1:8 [MPEA12–MPEA18] and 0:1 [(PEA)₂PbBr₄]) (Table S1, Supporting Information). Then, the perovskite solutions were spin-coated on glass/self-organized buffer hole injection layer (Buf-HIL) (50 nm) substrates.^[2] Perovskite films prepared from the mixed solutions showed several different distinctive peaks in their absorption spectra at room temperature (Figure 2a), which implies that the films consist of different quasi-2D perovskite crystals with diverse dimensions. The MAPbBr₃ film showed a peak near wavelength $\lambda = 540$ nm,^[2] and the (PEA)₂PbBr₄ film showed a peak near $\lambda = 395$ nm.^[11] However, quasi-2D perovskite films showed several different absorption peaks ($\lambda = 395$, 431, 450 nm), including these two. We assigned m for each peak: a monolayer ($m = 1$, $\lambda = 395$ nm), a bilayer ($m = 2$, $\lambda = 431$ nm), and a trilayer ($m = 3$, $\lambda = 450$ nm), and also 3D structure perovskite ($m \gg 4$, $\lambda = 540$ nm).^[12] As the proportion of (PEA)₂PbBr₄ in the precursor solution increased, the absorption peaks of $m = 1-3$ became dominant, which indicate the proportions of the 2D and quasi-2D perovskites increased.

From steady-state PL, the peaks had similar positions in all quasi-2D perovskite films. All quasi-2D perovskite films had PL $\lambda \approx 520$ nm, regardless of the MAPbBr₃:(PEA)₂PbBr₄ ratios in the precursor solutions; this result means that the PL comes only from the quasi-2D perovskite crystals with the

J. Byun, H. Cho, C. Wolf, Prof. T.-W. Lee
Department of Materials Science
and Engineering
Pohang University of Science and Technology
(POSTECH)
Pohang, Gyungbuk 37673, Republic of Korea
E-mail: twlee@postech.ac.kr; taewlees@gmail.com

Dr. M. Jang, Prof. H. Yang
Department of Applied Organic Materials Engineering
Inha University
Incheon 22212, Republic of Korea
Dr. A. Sadhanala, Prof. R. H. Friend
Cavendish Laboratory
University of Cambridge
JJ Thomson Avenue, Cambridge CB3 0HE, UK



DOI: 10.1002/adma.201601369

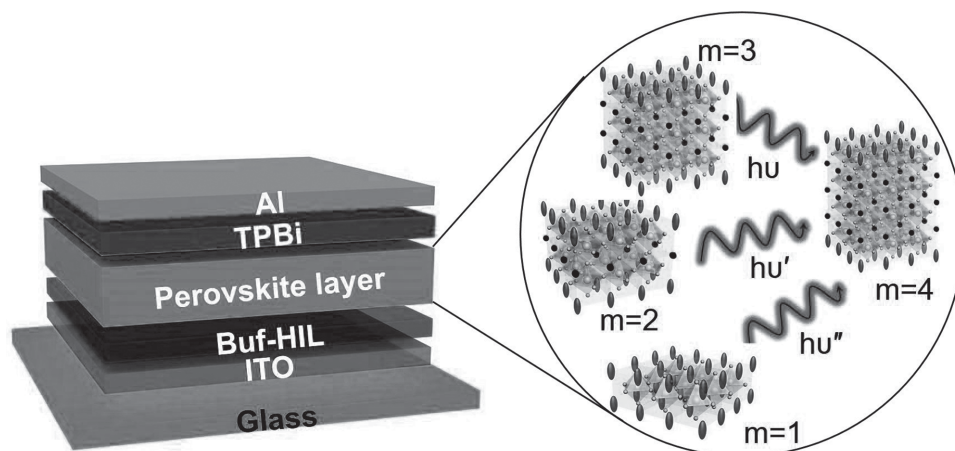


Figure 1. Schematic diagram of the quasi-2D PeLEDs structure.

smallest bandgap (the highest m) (Figure 2b, Figure S2 in the Supporting Information).

To investigate the crystal structure of perovskite films, we conducted grazing-incidence X-ray diffraction (GI-XRD)

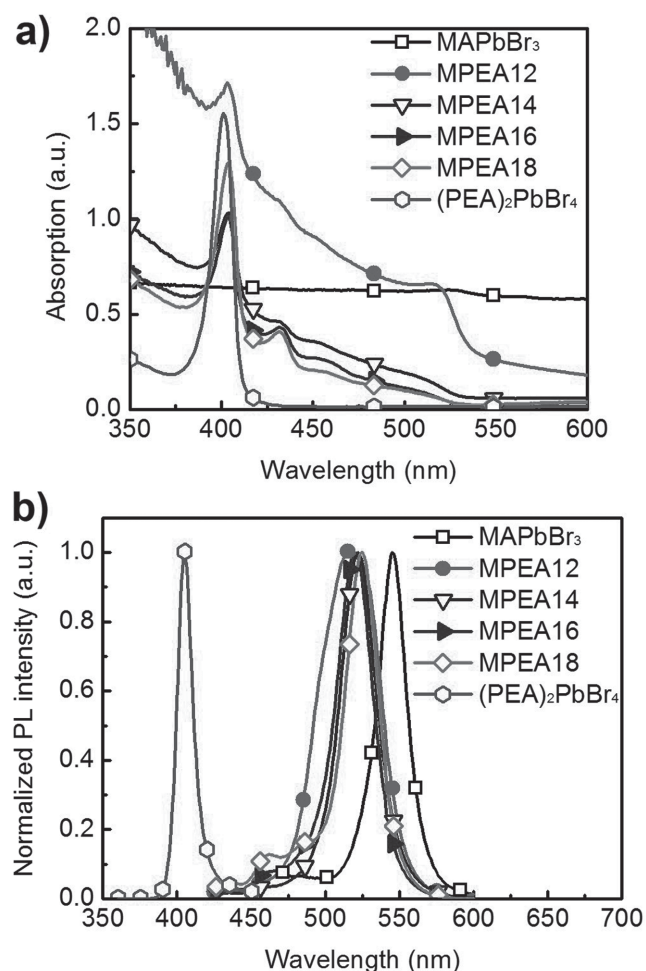


Figure 2. a) UV-vis absorption spectrum of quasi-2D perovskite films on glass substrate. b) PL spectrum of quasi-2D perovskite films on glass substrate (codes: Table S1, Supporting Information).

(Figure 3a–c, Figure S3a–f in the Supporting Information). As the proportion of $(\text{PEA})_2\text{PbBr}_4$ increases, the perovskite films showed ordered layer structure in out-of-plane direction. Also, the quasi-2D perovskite films had several peaks at 14.2° and 27.9° that MAPbBr_3 or $(\text{PEA})_2\text{PbBr}_4$ films did not show: they had different crystal structures compared to 3D or 2D perovskites (Figure 3d). The peaks at 14.2° and 27.9° correspond to 6.3 \AA d -spacing by Bragg's law. This indicates quasi-2D perovskite crystals include distorted octahedral inorganic structures (Figure S3, Supporting Information) because the d -spacing is larger than that of 3D structure perovskites in (001) plane (5.9 \AA). This can be also supported by the fact that 2D perovskites have distorted octahedral inorganic structures with size of $\approx 6.3 \text{ \AA}$ (Figure 3e).^[13] We can verify that all quasi-2D perovskite films have both aligned and distorted inorganic layers because it contains both 3D and quasi-2D perovskite crystals.

As the proportion of $(\text{PEA})_2\text{PbBr}_4$ in the precursor solution increased, the particle size of the perovskite film decreased (Figure S1, Supporting Information). Spontaneous crystallization of MAPbBr_3 on Buf-HIL formed non-uniform film morphology consisting of both thin uniform MAPbBr_3 film and scattered large particles which are $>1 \mu\text{m}$. Particles formed from MPEA12 were $<1 \mu\text{m}$, and in MPEA14–MPEA18 the particles were too small to be distinguished (Figure S1c–f, Supporting Information). The surfaces of all quasi-2D perovskite films were uniform without pinholes. The uniform film morphology and the decrease in particle size with increasing $(\text{PEA})_2\text{PbBr}_4$ proportion imply that quasi-2D PeLEDs can show enhanced luminescent characteristics with reduced electrical shunt paths and stronger spatial confinement of excitons.^[6]

We conducted time-correlated single-photon counting (TCSPC) with different perovskite films to investigate the effect of changes in crystal structure on PL lifetime (Figure 4a). We used the same sample structures as for steady-state PL measurement. PL decay curves were well described by tri-exponential decay fitting, except MAPbBr_3 and MPEA12; this relationship suggests that the PL decay of perovskite films occurred through three pathways. The pure $(\text{PEA})_2\text{PbBr}_4$ film had the shortest average PL lifetime (Table S2, Supporting Information). The fastest decay (τ_3), which was not shown in MAPbBr_3 and MPEA12, originates from $(\text{PEA})_2\text{PbBr}_4$ crystals. The

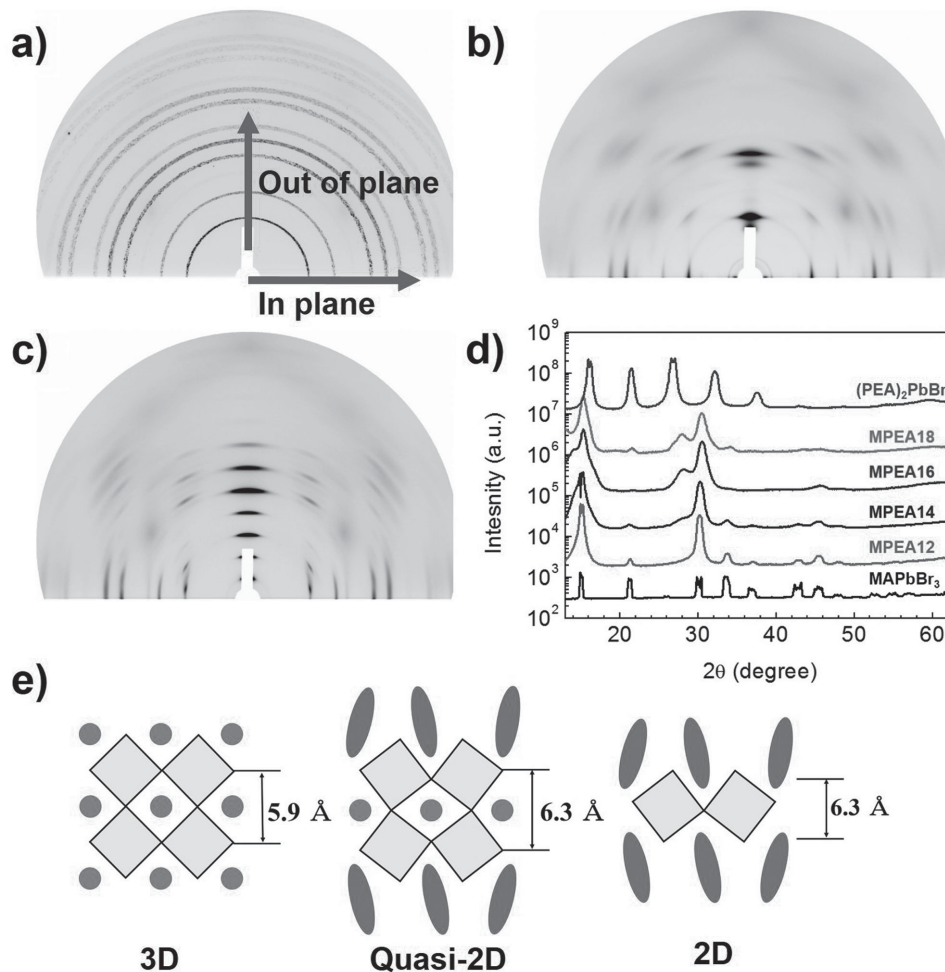


Figure 3. a–c) GI-XRD data of MAPbBr₃ (a), MPEA18 (b), (PEA)₂PbBr₄ (c), and d) 1D GI-XRD plot of out-of-plane direction. e) Schematic diagrams of 3D, quasi-2D, and 2D perovskite crystal structures (codes: Table S1, Supporting Information).

second-fastest PL decay (τ_2) is caused by trap-assisted recombination, and the slowest decay (τ_1) is related to radiative recombination (Table S2, Supporting Information).^[14] As the proportion of (PEA)₂PbBr₄ in the precursor increased from MPEA12 to MPEA18, the PL lifetime in the τ_1 and τ_2 increased, so average PL lifetime increased. Also, we conducted PLQE measurement to compare PLQE of the quasi-2D and 3D perovskite films. The quasi-2D perovskite film (MPEA16) showed a higher PLQE of 34%, while the MAPbBr₃ film showed very weak PL with very low PLQE (<2–3%).

The tDOS of PeLEDs was calculated from capacitance versus frequency measurement.^[15] The trap density was highest in MAPbBr₃; adding (PEA)₂PbBr₄ reduced tDOS over the entire energy range, and minimized it in MPEA16 (Figure 4b). Especially, deep traps were reduced as the proportion of (PEA)₂PbBr₄ increased (Figure 4b), which thereby reduces non-radiative trap-assisted recombination.^[16]

The performance (i.e., current density, luminance, and current efficiency) (Figure 5) was measured in quasi-2D PeLEDs that had ITO/Buf-HIL(50 nm)/perovskite/1,3,5-tris(*N*-phenylbenzimidazole-2-yl)benzene (TPBI) (50 nm)/LiF (1 nm)/Al (100 nm) structure. Because (PEA)₂PbBr₄ has a

slower charge-transport property than MAPbBr₃ due to long insulating OA chains between inorganic layers, increasing the proportion of PEA in quasi-2D perovskite films caused decrease in current density; current density was lowest at pure (PEA)₂PbBr₄. The PeLEDs that used quasi-2D perovskite films exhibited much higher current efficiency and luminance than PeLEDs that used 3D MAPbBr₃. The PeLED that used MPEA16 showed the best maximum luminance (2935 cd m⁻²) and current efficiency (4.90 cd A⁻¹) (Figure 5b,c). This can be attributed to: i) fully homogeneous perovskite films that formed with small particle size, ii) the lowest trap density, iii) the higher PLQE (34%) than MAPbBr₃ (<2–3%), and iv) decent charge transport property.

Mixing MAPbBr₃ and (PEA)₂PbBr₄ caused slight changes in the electroluminescence (EL) spectrum peaks of the PeLEDs (Figure 5d). The MAPbBr₃ PeLED had an EL peak at $\lambda = 540$ nm, and the pure (PEA)₂PbBr₄ PeLED had an EL peak at $\lambda = 405$ nm. A mixture of these two perovskites changed the EL wavelength to $510 \leq \lambda \leq 520$ nm. This is the same trend that was observed in the PL spectra. The analysis results of UV-vis absorption and GI-XRD indicate that each perovskite film is formed with two or three different crystal structures, and that

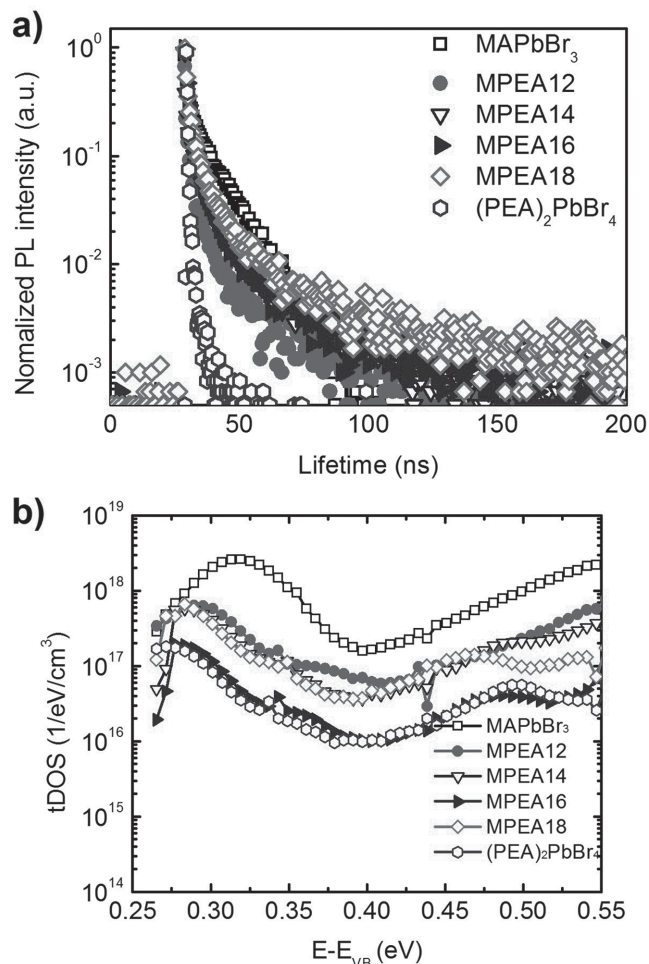


Figure 4. a) PL lifetime curves obtained from time-correlated single photon counting measurement of quasi-2D perovskite films. $\tau_{ave} = \sum(f_i \tau_i)$, where f_i are fractional intensities and τ_i are measured lifetimes. b) Trap density of state (tDOS) of quasi-2D PeLEDs. Each device has ITO/Buf-HIL(50 nm)/perovskite film/TPBI(50 nm)/LiF(1 nm)/Al(100 nm) structure (codes: Table S1, Supporting Information).

each structure has a distinct bandgap. However, all PL and EL are emitted by only one type of quasi-2D perovskite crystals that have the smallest bandgap close to that of MAPbBr₃. The excitation energy transfer among perovskite crystals with different bandgaps is a possible mechanism: the excitons generated in quasi-2D perovskite crystals with large bandgap ($m = 1-3$) migrate to the crystals with the smallest bandgap. As a result, emission spectra from the states with the smallest bandgap ($\lambda = 510-520$ nm) were observed.

In conclusion, our work successfully demonstrated that development of visible light-emitting quasi-2D perovskite materials instead of pure 3D and 2D perovskite materials can be a promising direction to achieve highly efficient visible PeLEDs. We developed quasi-2D perovskites by mixing PEA lead bromide ((C₆H₅C₂H₄NH₃)₂PbBr₄, (PEA)₂PbBr₄) with MAPbBr₃, which in turn leads to demonstration of high-efficiency solution-processed green PeLEDs with a simple device structure. We used several different precursor solutions with varying MA:PEA ratio. Because of enhancement of film quality, enhanced exciton

confinement, and reduced trap density, PeLEDs that used the quasi-2D perovskite materials as emission layers showed much higher current efficiency and luminance than those of PeLEDs that used 3D or 2D perovskite materials. The optimum device (i.e., MPEA16 device) showed the highest current efficiency and luminance: 4.90 cd A⁻¹ and 2935 cd m⁻², respectively.

However, in quasi-2D perovskites, a trade-off exists between losing electrical conductivity and obtaining advantages including the enhancement of film quality, exciton confinement, and reduced trap density. It is hard to solve this issue because of intrinsic low charge carrier mobility of 2D perovskites (here, (PEA)₂PbBr₄). We think this issue can be solved by finding an appropriate 2D perovskite incorporating OA cations that are smaller and have higher charge carrier mobility than PEA, while maintaining 2D perovskite structures.

Experimental Section

Organic Ammonium Bromide Synthesis: Precursor materials (phenylethylamine, methylamine solution, and hydrobromic acid) were purchased from Sigma-Aldrich. To synthesize OA bromide, both methylamine solution and phenylethylamine were mixed with hydrobromic acid with the 1:1 (mol:mol) ratio at 0 °C; this reaction takes >4 h. The resulting white precipitate was collected by evaporating the solvent, then purified by dissolving in ethanol, recrystallizing from diethyl ether, and drying at 80 °C in a vacuum oven for 12 h.

PeLED Device Fabrication: Substrates coated with indium tin oxide were sonicated sequentially in acetone and isopropyl alcohol for 15 min each, then boiled in isopropyl alcohol for 15 min to remove residues, and dried using an N₂ gun. Substrates were exposed to UV light for 15 min for ozone treatment, then a Buf-HIL solution (poly(3,4-ethylenedioxythiophene):poly(styrene sulfonate):perfluorinated ionomer = 1:6:25.4 (w:w:w)) was spin-coated on the substrate and annealed at 150 °C for 30 min. Spin-coating of perovskite layers was performed in N₂ atmosphere.^[2]

Two precursor solutions were made, MAPbBr₃ (40 wt%) and (PEA)₂PbBr₄ (10 wt %) in DMF solvent. The solutions were mixed in ratios of 1:0, 1:2, 1:4, 1:6, 1:8, and 0:1 (vol:vol), then spin-coated on the ITO/Buf-HIL substrate, and annealed at 90 °C for 10 min. TPBI (50 nm)/LiF (1 nm)/Al (100 nm) were deposited on the perovskite films by vacuum deposition in thermal evaporator under high vacuum (<10⁻⁶ Torr).

Photoluminescence (PL) Measurement: PL spectra were measured using a JASCO FP6500 spectrofluorometer.

GI-XRD Measurement: GI-XRD measurement was conducted at beamlines 3C, 6D, and 9A at the Pohang Accelerator Laboratory (PAL), Korea. Perovskite films were spin-coated on a Buf-HIL-coated Si wafer. An X-ray with $\lambda = 0.62382$ Å and incidence angle = 0.1° was^[3] used in this study.

PeLED Characterization: The current-voltage-luminance characteristics were measured using a Keithley 236 source measurement and a Minolta CS2000 spectroradiometer.

Time-Correlated Single Photon Counting (TCSPC) Measurement: PL decays of various perovskites were quantified using TCSPC measurement. Two different excitation lasers were used in this study, one with $\lambda = 375$ nm (used to measure pure (PEA)₂PbBr₄ films) and the other with $\lambda = 405$ nm (used to measure other perovskite films). All perovskite films were capped with poly(methyl methacrylate).

Trap Density of State (tDOS) Measurement and Calculation: The tDOSs were calculated from capacitance versus frequency measurements according to Carr et al.^[15] The frequency-dependent capacitance $C_p(f)$ was measured using a Bio-Logic SP300 potentiostat in the frequency range from 1 Hz to 7 MHz, 0 V DC, and 25 mV AC amplitude. Depletion width and built-in potential was calculated from Mott-Schottky plots at 1 kHz. Assuming an attempt-to-escape frequency of $\omega_0 = 10^{12}$ s⁻¹, the frequency was converted into an energy scale by Equation (1):

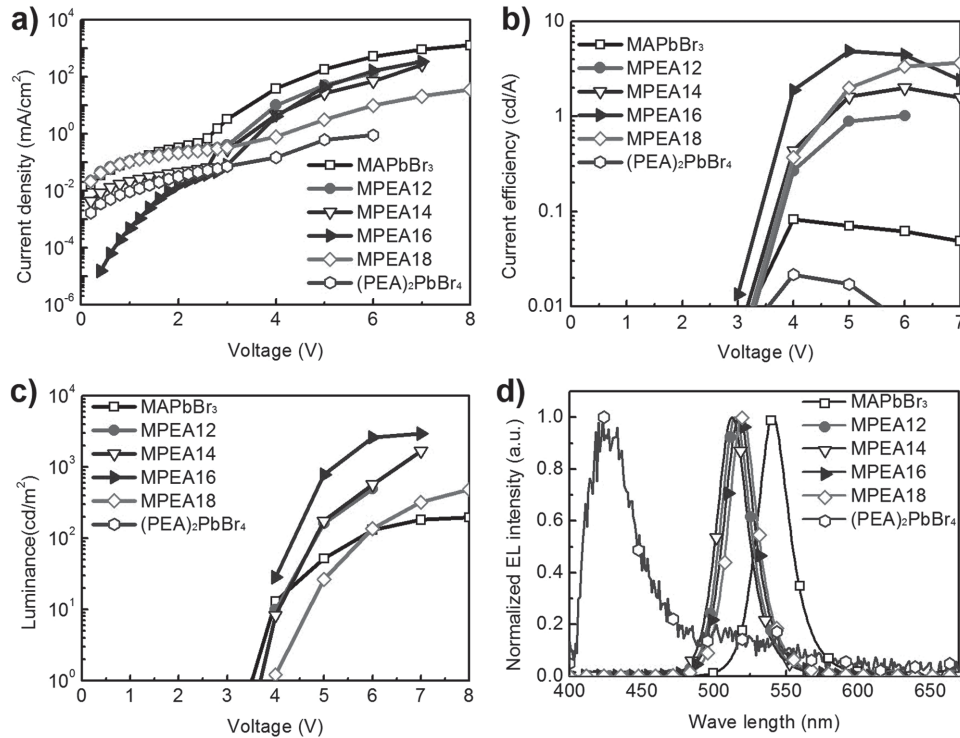


Figure 5. Performance of quasi-2D PeLEDs with ITO/Buf-HIL (50 nm)/perovskite film/TPBI (50 nm)/LiF (1 nm)/Al (100 nm) structure: a) current density versus voltage; b) current efficiency versus voltage; c) luminance versus voltage; d) normalized EL spectra (codes: Table S1, Supporting Information).

$$E_{\omega} = k_B T \ln \frac{\omega_0}{\omega} \quad (1)$$

The tDOS spectrum was calculated by:

$$N_T(E_{\omega}) = -\frac{V_{bi}}{qW} \frac{dC_p}{d\omega} \frac{\omega}{k_B T} \quad (2)$$

where V_{bi} is the built-in potential, qW is the electron charge times the depletion width, and $\omega = 2\pi f$ is the frequency; $k_B T$ is the thermal energy.

Note that the trap energy level (x -axis in Figure 5b) was depicted in a relative energy scale due to the assumption about ω_0 .

Supporting Information

Supporting Information is available from the Wiley Online Library or from the author.

Acknowledgements

J.B. and H.C. contributed equally to this work. This research was supported by the Nano Material Technology Development Program through the National Research Foundation of Korea (NRF) funded by the Ministry of Science, ICT & Future Planning (MSIP, Korea) (NRF-2014M3A7B4051747). A.S. and R.H.F. would like to acknowledge support from EPSRC and the India-UK APEX project. H.Y. would like to acknowledge support from the General Research Program (2013R1A12063963) of the Ministry of Education, Science, and Technology.

Received: March 10, 2016

Revised: May 6, 2016

Published online: June 23, 2016

- a) Z.-K. Tan, R. S. Moghaddam, M. L. Lai, P. Docampo, R. Higler, F. Deschler, M. Price, A. Sadhanala, L. M. Pazos, D. Credgington, F. Hanusch, T. Bein, H. J. Snaith, R. H. Friend, *Nat. Nanotechnol.* **2014**, *9*, 687; b) J. C. Yu, D. B. Kim, G. Baek, B. R. Lee, E. D. Jung, S. Lee, J. H. Chu, D.-K. Lee, K. J. Choi, S. Cho, M. H. Song, *Adv. Mater.* **2015**, *27*, 3492; c) A. Sadhanala, S. Ahmad, B. Zhao, N. Giesbrecht, P. M. Pearce, F. Deschler, R. L. Z. Hoyer, K. C. Gödel, T. Bein, P. Docampo, S. E. Dutton, M. F. L. De Volder, R. H. Friend, *Nano Lett.* **2015**, *15*, 6095; d) R. L. Z. Hoyer, M. R. Chua, K. P. Musselman, G. Li, M.-L. Lai, Z.-K. Tan, N. C. Greenham, J. L. MacManus-Driscoll, R. H. Friend, D. Credgington, *Adv. Mater.* **2015**, *27*, 1414; e) G. Li, Z.-K. Tan, D. Di, M. L. Lai, L. Jiang, J. H.-W. Lim, R. H. Friend, N. C. Greenham, *Nano Lett.* **2015**, *15*, 2640; f) J. C. Yu, D. B. Kim, E. D. Jung, B. R. Lee, M. H. Song, *Nanoscale* **2016**, *8*, 7036.
- Y.-H. Kim, H. Cho, J. H. Heo, T.-S. Kim, N. Myoung, C.-L. Lee, S. H. Im, T.-W. Lee, *Adv. Mater.* **2015**, *27*, 1248.
- a) K.-G. Lim, S. Ahn, Y.-H. Kim, Y. B. Qi, T.-W. Lee, *Energy Environ. Sci.* **2016**, *9*, 932; b) K.-G. Lim, S. Ahn, H. Kim, M.-R. Choi, D. H. Huh, T.-W. Lee, *Adv. Mater.* **2016**, *3*, 1500678; c) H. Kim, K. G. Lim, T.-W. Lee, *Energy Environ. Sci.* **2016**, *9*, 12.
- a) S. D. Stranks, G. E. Eperon, G. Grancini, C. Menelaou, M. J. P. Alcocer, T. Leijtens, L. M. Herz, A. Petrozza, H. J. Snaith, *Science* **2013**, *342*, 341; b) Y. Yang, M. Yang, Z. Li, R. Crisp, K. Zhu, M. C. Beard, *J. Phys. Chem. Lett.* **2015**, *6*, 4688.
- a) K. Tanaka, T. Takahashi, T. Ban, T. Kondo, K. Uchida, N. Miura, *Solid State Commun.* **2004**, *127*, 619; b) A. Miyata, A. Mitioglu, P. Plochocka, O. Portugall, J. T.-W. Wang, S. D. Stranks, H. J. Snaith, R. J. Nicholas, *Nat. Phys.* **2015**, *11*, 582.
- H. Cho, S.-H. Jeong, M.-H. Park, Y.-H. Kim, C. Wolf, C.-L. Lee, J. H. Heo, A. Sadhanala, N. Myoung, S. Yoo, S. H. Im, R. H. Friend, T.-W. Lee, *Science* **2015**, *350*, 1222.
- D. B. Mitzi, *J. Chem. Soc., Dalton Trans.* **2001**, *1*.

- [8] a) T. Goto, H. Makino, T. Yao, C. H. Chia, T. Makino, Y. Segawa, G. A. Mousdis, G. C. Papavassiliou, *Phys. Rev. B* **2006**, 73, 115206; b) O. Yaffe, A. Chernikov, Z. M. Norman, Y. Zhong, A. Velauthapillai, A. van der Zande, *Phys. Rev. B* **2015**, 92, 045414.
- [9] a) I. C. Smith, E. T. Hock, D. Solis-Ibarra, M. D. McGehee, H. I. Karunadasa, *Angew. Chem.* **2014**, 126, 11414; b) Z. Yuan, Y. Shu, Y. Xin, B. Ma, *Chem. Commun.* **2016**, 52, 3887; c) L. N. Quan, M. Yuan, R. Comin, O. Voznyy, E. M. Beauregard, S. Hoogland, A. Buin, A. R. Kirmani, K. Zhao, A. Amassian, D. H. Kim, E. H. Sargent, *J. Am. Chem. Soc.* **2016**, 138, 2649.
- [10] K. Tanaka, T. Kondo, *Sci. Technol. Adv. Mater.* **2003**, 4, 599.
- [11] K. Jemli, P. Audebert, L. Galmiche, G. Trippe-Allard, D. Garrot, J.-S. Lauret, E. Deleporte, *ACS Appl. Mater. Interfaces* **2015**, 7, 21763
- [12] Y. Tabuchi, K. Asai, M. Rikukawa, K. Sanui, K. Ishigure, *J. Phys. Chem. Solids* **2000**, 61, 837.
- [13] T. Ishihara, J. Takahashi, T. Goto, *Phys. Rev. B* **1990**, 42, 11099.
- [14] P.-W. Liang, C.-Y. Liao, C.-C. Chueh, F. Zuo, S. T. Williams, X.-K. Xin, J. Lin, A. K.-Y. Jen, *Adv. Mater.* **2014**, 26, 3748.
- [15] J. A. Carr, S. Chaudhary, *Energy Environ. Sci.* **2013**, 6, 3414.
- [16] G.-J. A. H. Werzelaer, M. Scheepers, A. M. Sempere, C. Momblona, J. Avila, H. J. Bolink, *Adv. Mater.* **2015**, 27, 1837.